Electronic Supplementary Material (ESI) for CrystEngComm.
This journal is © The Royal Society of Chemistry 2020

The affinity of copper(II) ions towards L-amino acids in the solid-state: a simple route towards mixed complexes

Kristina Smokrović,[a] Ivica Đilović*[a] and Dubravka Matković - Čalogović[a]

July 1, 2020

[a] University of Zagreb, Faculty of Science, Department of Chemistry, Horvatovac 102a, HR-10000 Zagreb, Croatia

Corresponding authors:

[*] E-mail: ivica.djilovic@chem.pmf.hr

Contents

1 Synthesis

1.1 In solution

Copper(II) hydroxide was prepared from the aqueous solution of tetraamminecopper(II) sulfate by precipitation with sodium hydroxide.[1,2]

Single complexes, Cu(aa)$_2$

Freshly prepared copper(II) hydroxide (1.00 mmol, 97.6 mg) and the desired amino acid (2.00 mmol, table Table S1), were added to 5.0 mL of distilled water. The resulting mixture is heated and stirred for 2 h at 90 °C, and left to cool down to room temperature (**??** Scheme S1).*

In the case of low solubility(L-Phe, L-Trp, L-Gln and L-Asn) of the complex the prepared sample can be simply filtered off and washed out with a dilute aqueous solution of sodium hydroxide (10%) to remove excess of unreacted amino acid. For the complexes that are readily soluble(L-His and L-Pro), 5.0 mL of ethanol (96%) should be added as precipitant. The resulting dark blue solution is then reduced to the half of the initial volume and left in a cool and dark place until the complex precipitates.

Mixed complexes, Cu(aa1)(aa2)

Freshly prepared copper(II) hydroxide (1.00 mmol, 97.6 mg) and an equimolar amount (1.00 mmol, masses are listed in table Table S1), of each amino acid (**aa1** and **aa2**) are added to 5.0 mL of distilled water. The resulting mixture was heated and stirred for 2 h at 90 °C, and left to cool down to room temperature.

Table S1: Mass of each amino acid used in solution synthesis of Cu(**aa**)$_2$ (2^{nd} column) and Cu(**aa1**)(**aa2**)(3^{rd} column) complexes.

	m(**aa**)/mg	
aa	Cu(**aa**)$_2$	Cu(**aa1**)(**aa2**)
L-Phe	330.38	165.19
L-Trp	408.46	204.23
L-His	310.32	155.16
L-Pro	230.26	115.13
L-Gln	292.30	146.15
L-Asn	264.24	132.12

1.2 Mechanochemical synthesis

All milling experiments were made in the Retsch MM 200 using two 7 mm steel balls (1.4 g each) in the poly(methyl)methacrylate (PMMA, or Plexiglas) 14 mL jar, at 25 Hz for 30 min. For liquid-assisted grinding experiments 40 µL of 50 % ethanol mixture (η-values in table Table S2) was added to the reactants.

Table S2: η-values for 50% aqueous ethanol solution used for the LAG experiments.

η/ µL mg^{-1}	L-Phe	L-Trp	L-His	L-Pro	L-Gln	L-Asn
L-Phe	0.093	0.048	0.054	0.061	0.056	0.058
L-Trp		0.079	0.049	0.054	0.050	0.052
L-His			0.098	0.063	0.057	0.060
L-Pro				0.122	0.065	0.068
L-Gln					0.103	0.061
L-Asn						0.111

*We tried the same procedure using L-Trp and copper salts that contain poorly coordinating anions (such as perchlorate or nitrate anions). The amino acid was dissolved in an aqueous solution containing an equimolar amount of sodium hydroxide. This solution was then cooled and the solution of the copper(II) salt was added stepwise and with stirring, otherwise precipitation of copper(II) oxide occured. For the reasons we already discussed in the manuscript, we decided not to use other salts in both synthetic approaches.

Neat or liquid-assisted grinding (NG and LAG) of reactants, a single type of **aa** and freshly prepared copper(II) hydroxide in 2:1 molar ratio, resulted in the formation of the corresponding Cu(**aa**)$_2$ complexes. As evidenced by the analysis of the PXRD patterns (Figures S2-S7), products were obtained in high yield.

For competitive milling experiments, the stoichiometry of 1:2:2 molar ratio of the reactants (Cu(OH)$_2$, **aa1**, and **aa2** respectively) was used. This stoichiometry results in three possible outcomes. In the first outcome, one amino acid is preferred and the PXRD analysis shows a Cu(**aa1**)$_2$ complex and unreacted **aa2**. In the second possible outcome a mixed complex Cu(**aa1**)(**aa2**) is formed, both amino acids can be observed in the powder diffraction pattern. In the third possible, and the most complicated, case both Cu(**aa1**)$_2$ and Cu(**aa2**)$_2$ are present as well as each amino acid. In this case molar ratio of resulting complexes does not have to be 1, since the affinity of each amino acid towards copper(II) is not equal.

1.3 Comparison of mechanochemical and solution synthesis protocol

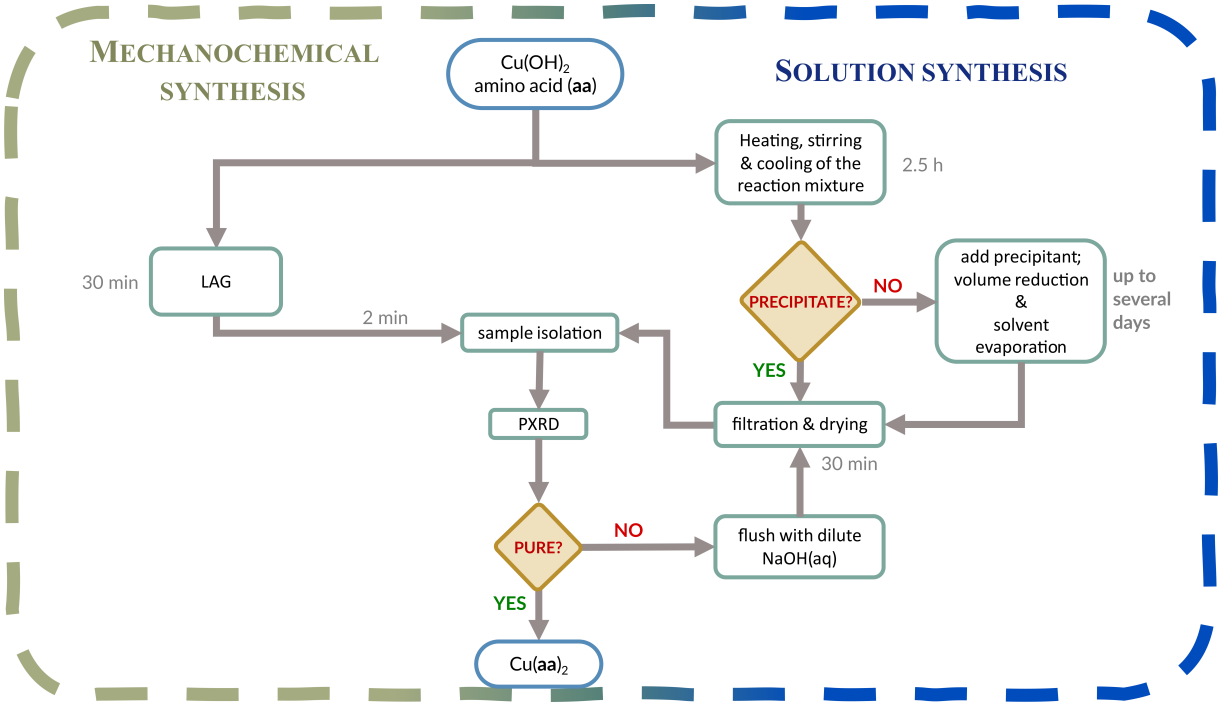

Scheme S1: Schematic overview of mechanochemical and solution synthesis of Cu(**aa**)$_2$ complexes.

2 Crystallographic data for the compound Cu(L-His)(L-Pro) · 2 H_2O

2.1 Asymmetric unit

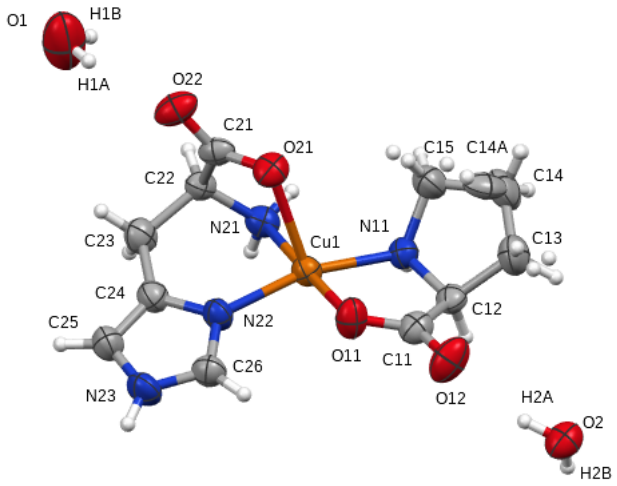

Figure S1: ORTEP plot of an asymmetric unit of Cu(L-His)(L-Pro) · 2 H_2O with the atom labeling scheme. Thermal ellipsoids are plotted at a 50 % probability. Hydrogen atoms are drawn as white spheres of arbitrary size.

Table S3: Selected bond lengths for Cu(L-His)(L-Pro)

Atom 1	Atom 2	Bond Length (Å)
Cu1	O11	1.950(4)
O21	Cu1	2.285(3)
Cu1	N22	1.978(4)
Cu1	N21	2.000(4)
Cu1	N11	2.005(3)

Table S4: Selected bond angles for Cu(L-His)(L-Pro)

Atom1	Atom2	Atom3	Angle (°)
N21	Cu1	N11	95.37(14)
N11	Cu1	O21	104.90(16)
N21	Cu1	O21	76.13(12)
O11	Cu1	N11	83.47(14)
O11	Cu1	N21	178.76(15)
O11	Cu1	N22	91.09(14)
O11	Cu1	O21	103.73(13)
N22	Cu1	N11	164.31(15)
N22	Cu1	N21	90.14(14)
N22	Cu1	O21	90.67(13)
C12	N11	Cu1	109.7(2)
C15	N11	Cu1	116.5(3)

Table S5: List of hydrogen bond parameters for Cu(L-His)(L-Pro)

Donor	Acceptor	D-H (Å)	H...A (Å)	D...A (Å)	D-H...A (°)	Type
N11-H11	O12	0.98	2.341	3.002	124.0	intermolecular
N11-H11	O22	0.98	2.589	3.360	135.6	intermolecular
N21-H21A	O21	0.89	2.717	3.359	130.0	intermolecular
N21-H21A	O2	0.89	2.401	3.173	145.2	intermolecular
N21-H21B	O2	0.89	2.071	2.935	163.5	intermolecular
N23-H23	O22	0.86	2.088	2.873	151.4	intermolecular
O2-H2A	O12	0.85	1.900	2.734	166.4	intermolecular
O2-H2B	O21	0.85	1.900	2.743	171.3	intermolecular
O1-H1A	O22	0.85	2.081	2.880	156.4	intermolecular
O1-H1B	O11	0.85	2.357	2.997	132.4	intermolecular
O1-H1B	O12	0.85	2.479	3.221	146.4	intermolecular

2.2 Table of crystallographic information

Table S6: Crystal data and structure refinement for Cu(L-His)(L-Pro)

Compound	Cu(L-His)(L-Pro)$\cdot 2\,H_2O$
Empirical formula	$C_{11}H_{20}CuN_4O_6$
Formula weight	367.85
Temperature/ K	293(2)
Crystal system	monoclinic
Space group	$P2_1$
a/ Å	9.7066(6)
b/ Å	8.1806(4)
c/ Å	10.3710(6)
α/ °	90
β/ °	114.199(7)
γ/ °	90
Volume/ Å^{-3}	751.15(8)
Z	2
ρ_{calc} / g/cm^{-3}	1.626
μ/ mm^{-1}	1.489
$F(000)$	382.0
Crystal size/ mm	0.333 × 0.286 × 0.094
Radiation	MoKα (λ = 0.71073Å)
2θ range for data collection/°	8.416 to 53.98
Index ranges	$-12 \leq h \leq 12$ $-10 \leq k \leq 10$ $-13 \leq l \leq 12$
Reflections collected	6231
Independent reflections	3261 [R_{int} = 0.0323, R_σ = 0.0460]
Data/restraints/parameters	3261/2/214
Goodness-of-fit on F^2	1.027
Final R indexes [$I \geq 2\sigma(I)$]	R_1 = 0.0334, wR_2 = 0.0781
Final R indexes [all data]	R_1 = 0.0403, wR_2 = 0.0815
Largest diff. peak/hole / e /Å^{-3}	0.58/ −0.29
Flack parameter	−0.003(10)

2.3 Crystal structure solution

The crystal and molecular structures of the complex [Cu(L−His)(L−Pro)]$\cdot 2H_2O$ (table Table S6) were determined using single-crystal X-ray diffraction data collected at room temperature. Diffracted intensities were collected on an Oxford Diffraction Xcalibur diffractometer with Sapphire3 CCD detector using graphite-monochromatic MoK_α radiation. Data sets were collected using ϕ-scans. CrysAlisPro system software[3] was used for data collection, cell refinement, and data reduction.

The structure of the synthesised compound was solved by direct methods and refined using the SHELXT[4] and SHELXL[5] programs, respectively. The refinement procedure by full-matrix least squares methods based on F^2 values against all reflections included anisotropic displacement parameters for all non-H atoms. Proline side-chain disorder was modelled in two positions(major part with 68.11% occupancy and 31.89% for the minor part). The positions of H-atom's each riding on carbon and nitrogen atoms were determined on stereochemical grounds. Hydrogen atoms on water molecules were modelled using distance restraints (DFIX), and oriented with H-O bonds oriented towards the closest, chemically reasonable hydrogen bond acceptor.

The SHELX programs were operated within the Olex2 crystallographic suite[6]. Geometrical calculations and molecular graphics were done with PLATON[7], MERCURY[8], and PYMOL[9]. Supplementary crystallographic data sets for the structure are available through the Cambridge Structural Data base with deposition number 1999476.

Copy of this information may be obtained free of charge from the director, CCDC, 12 Union Road, Cambridge, CB2 1EZ, UK (fax: +44 1223 336 033; email: deposit@ccdc.cam.ac.uk or http://www.ccdc.cam.ac.uk).

3 PXRD data analysis

PXRD data for as-synthesized samples was collected on PANalytical Aeris diffractometer (Bragg-Brentano geometry, zero background sample holder, Ni-filtered CuK radiation with the X-ray tube operating 7.5 mA and 40 kV). Diffractograms were visualized using *ggplot2* package[10] in R-Studio[11] program suite.

3.1 PXRD data for the complexes of $[Cu(aa)_2]$ type

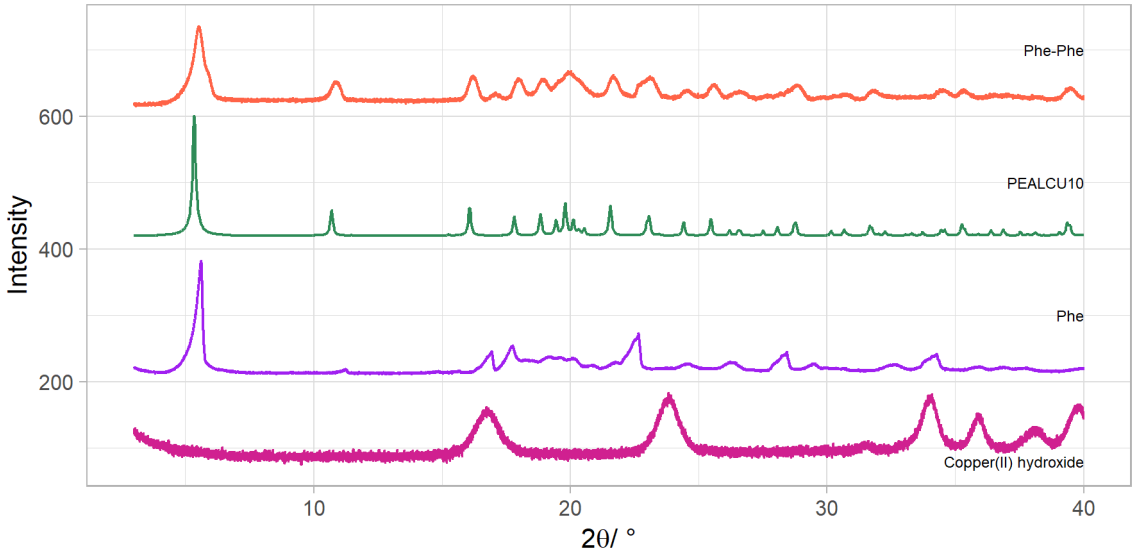

Figure S2: PXRD patterns of mechanochemically prepared samples of L-Phe with $Cu(OH)_2$ compared to the calculated patterns derived from the belonging CSD entries(refcode).

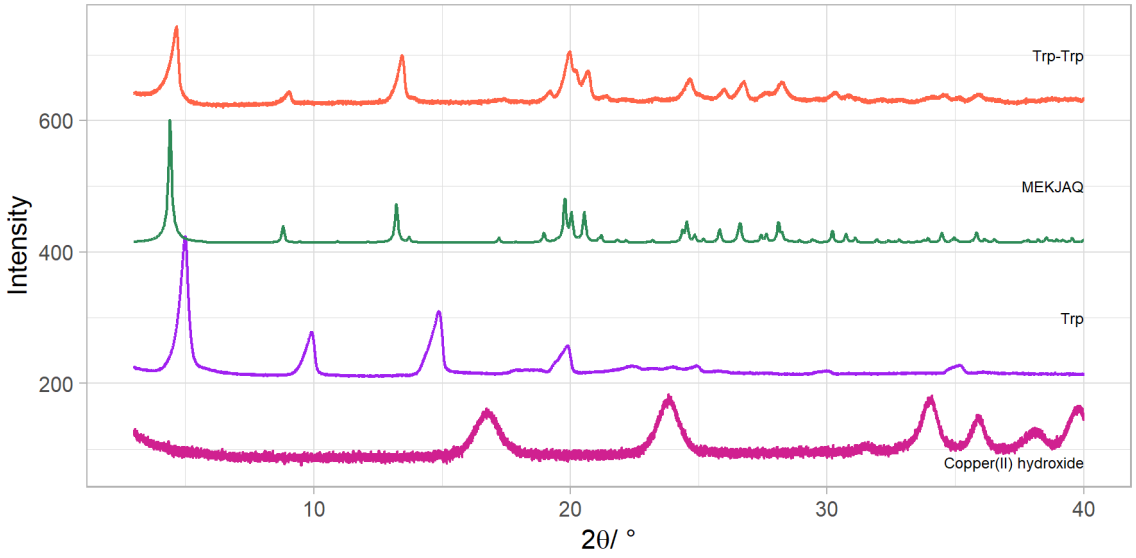

Figure S3: PXRD patterns of mechanochemically prepared samples of L-Trp with $Cu(OH)_2$ compared to calculated patterns derived from the belonging CSD entries(refcode).

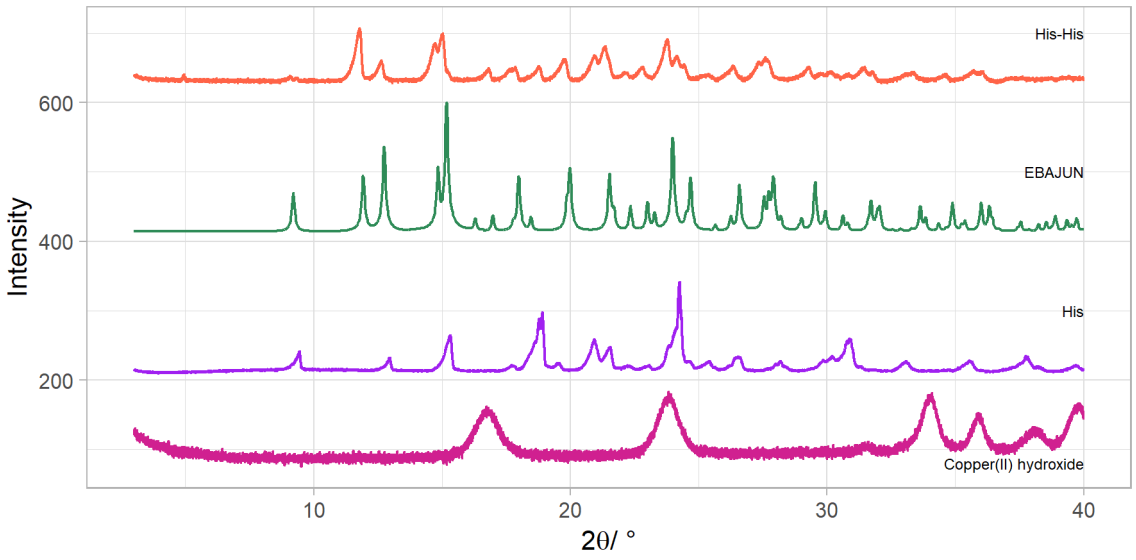

Figure S4: PXRD patterns of mechanochemically prepared samples of L-His with $Cu(OH)_2$ compared to calculated patterns derived from the belonging CSD entries(refcode).

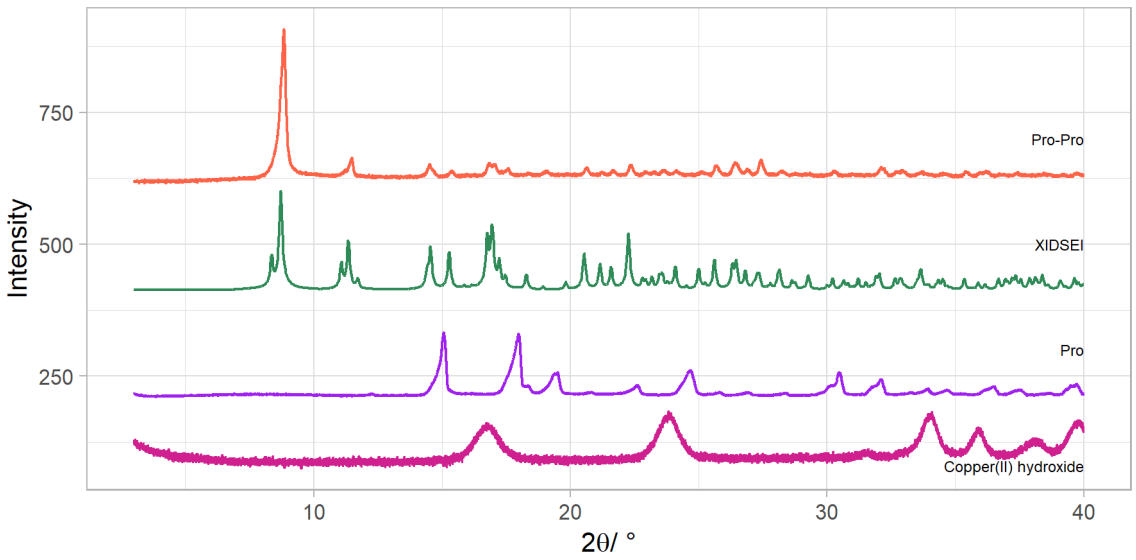

Figure S5: PXRD patterns of mechanochemically prepared samples of L-Pro with $Cu(OH)_2$ compared to calculated patterns derived from the belonging CSD entries(refcode).

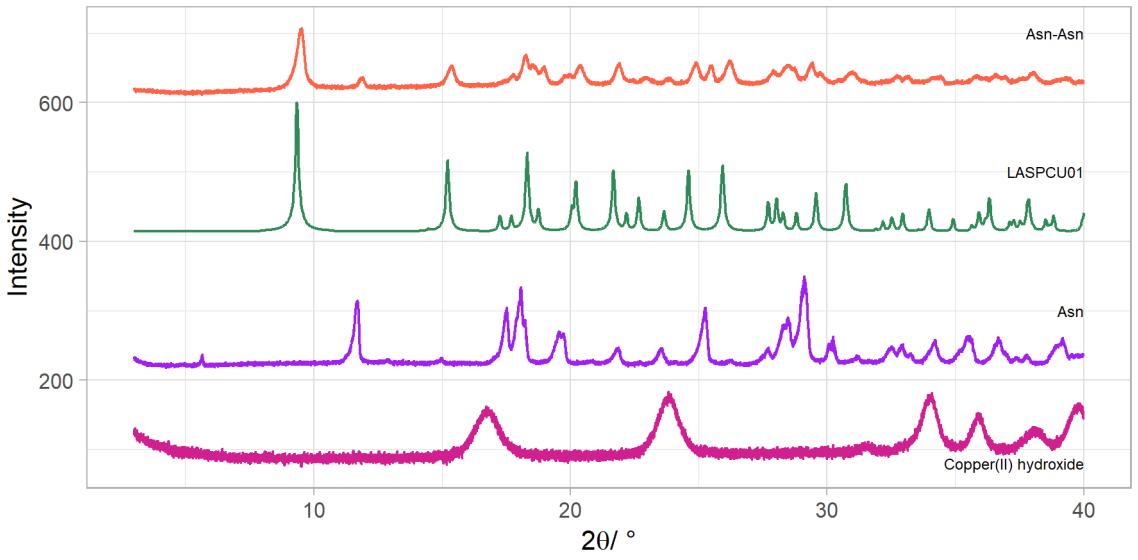

Figure S6: PXRD patterns of mechanochemically prepared samples of L-Asn with $Cu(OH)_2$ compared to calculated patterns derived from the belonging CSD entries(refcode).

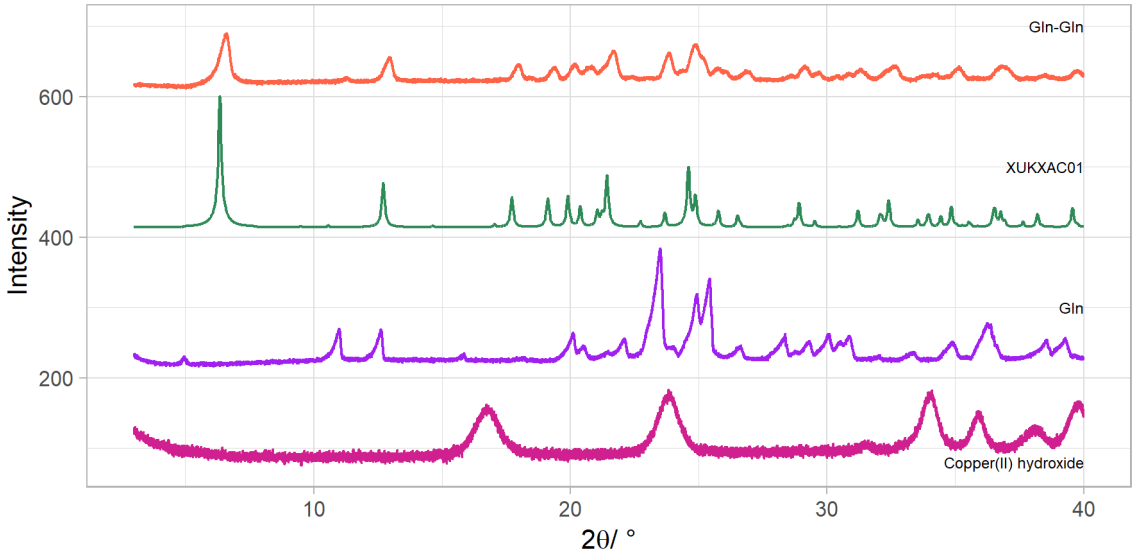

Figure S7: PXRD patterns of mechanochemically prepared samples of L-Gln with $Cu(OH)_2$ compared to calculated patterns derived from the belonging CSD entries(refcode).

3.2 PXRD data for the complexes of [Cu(aa1)(aa2)] type

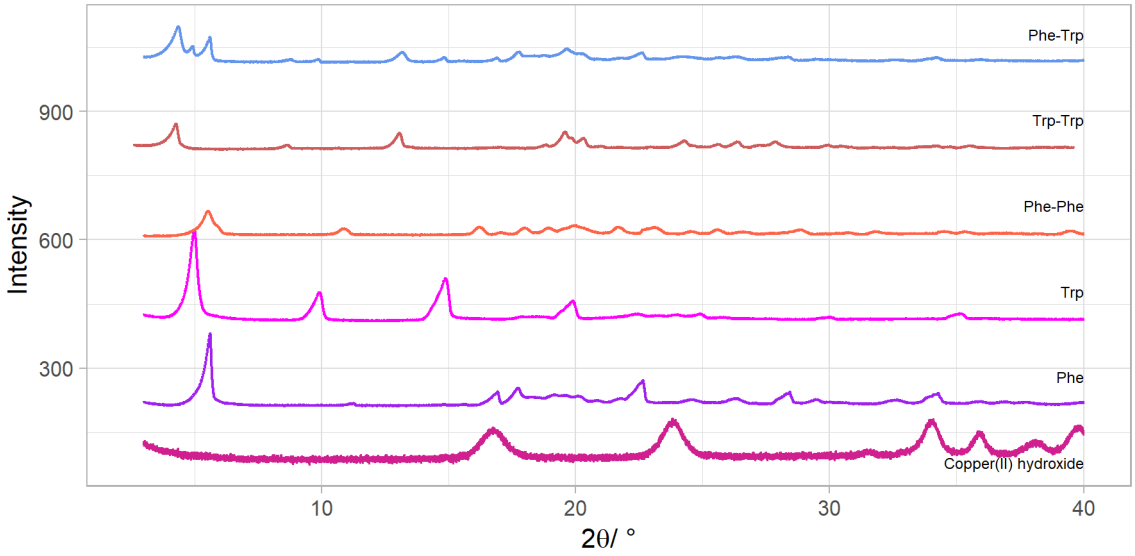

Figure S8: PXRD patterns of mechanochemically prepared samples of L-Phe and L-Trp with $Cu(OH)_2$ compared to calculated patterns derived from the belonging CSD entries(refcode).

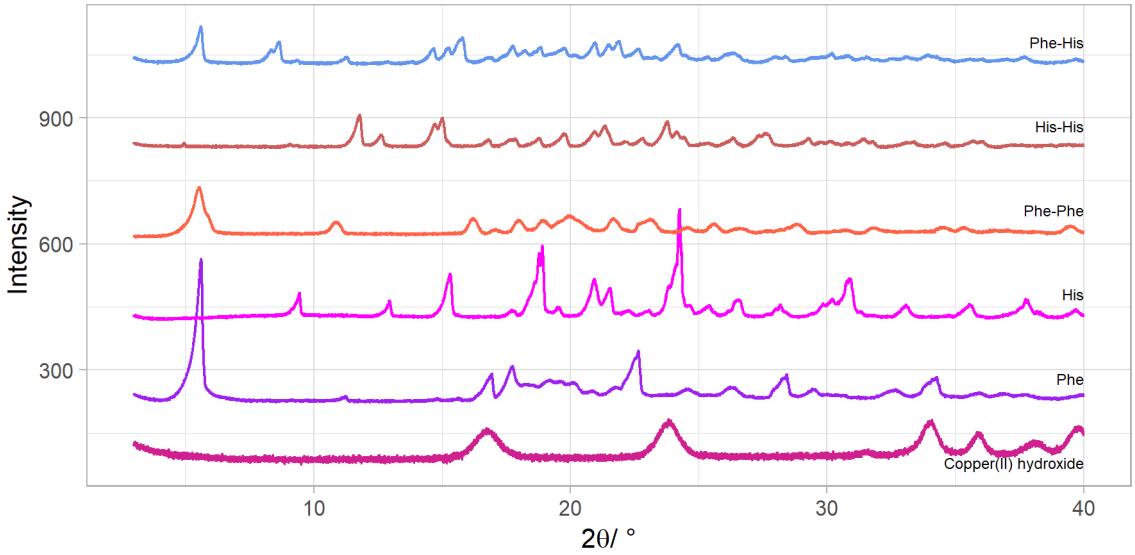

Figure S9: PXRD patterns of mechanochemically prepared samples of L-Phe and L-His with $Cu(OH)_2$ compared to calculated patterns derived from the belonging CSD entries(refcode).

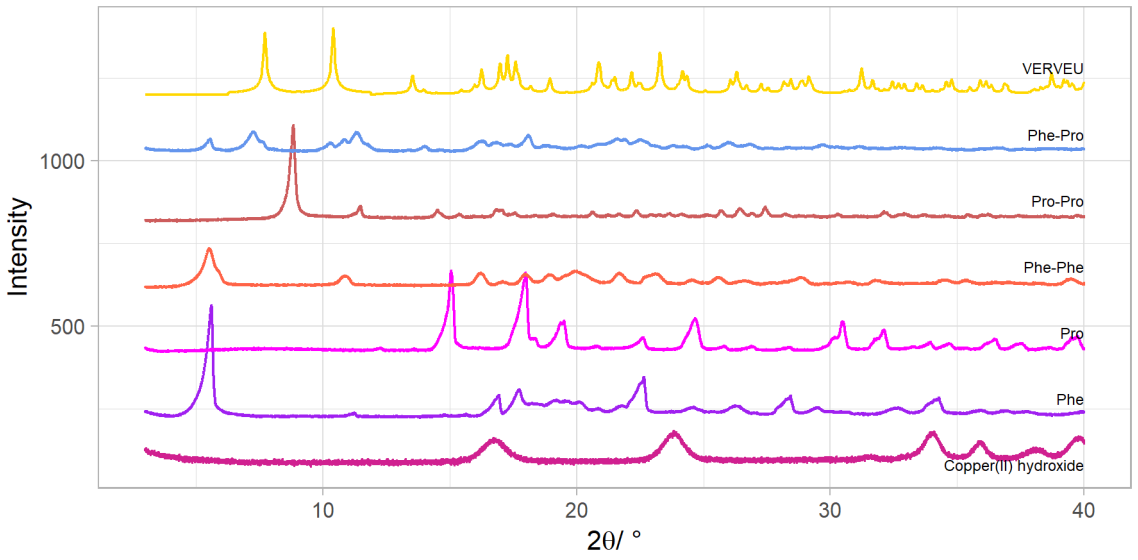

Figure S10: PXRD patterns of mechanochemically prepared samples of L-Phe and L-Pro with $Cu(OH)_2$ compared to calculated patterns derived from the belonging CSD entries(refcode).

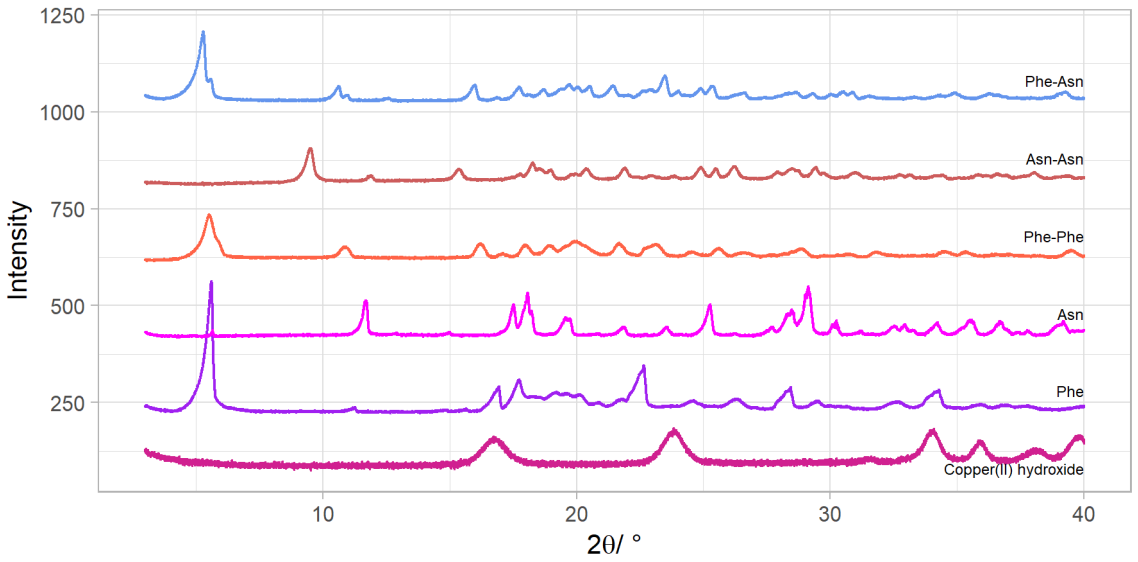

Figure S11: PXRD patterns of mechanochemically prepared samples of L-Phe and L-Asn with $Cu(OH)_2$ compared to calculated patterns derived from the belonging CSD entries(refcode).

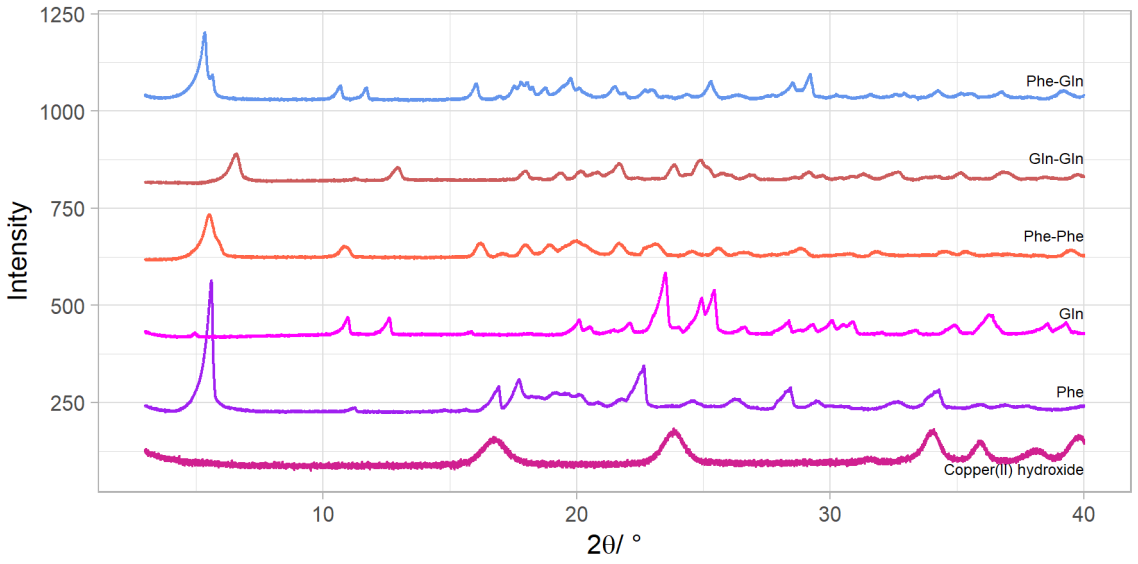

Figure S12: PXRD patterns of mechanochemically prepared samples of L-Phe and L-Gln with $Cu(OH)_2$ compared to calculated patterns derived from the belonging CSD entries(refcode).

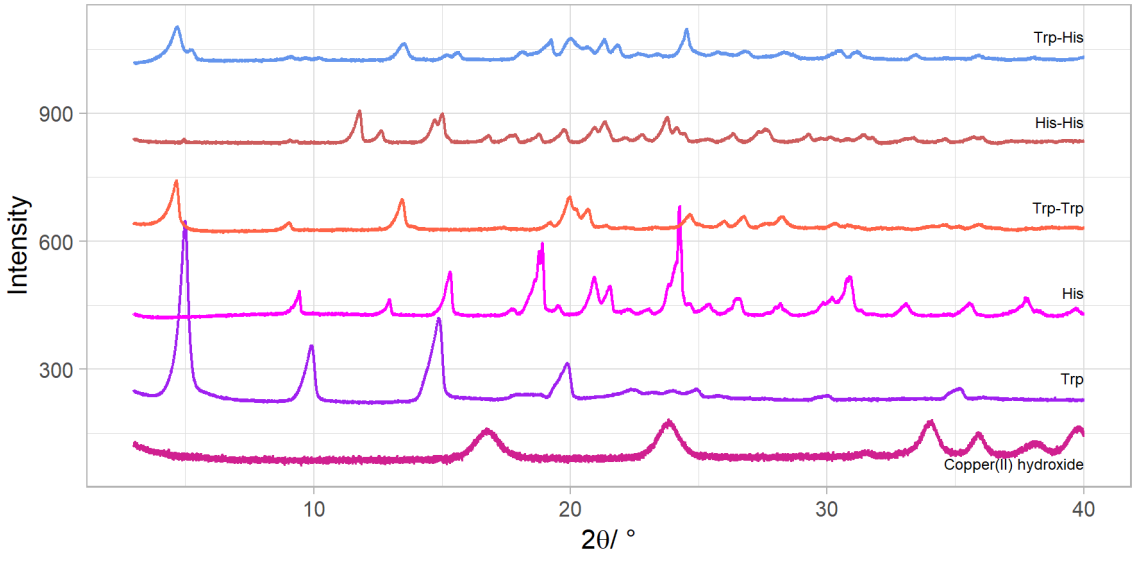

Figure S13: PXRD patterns of mechanochemically prepared samples of L-Trp and L-His with $Cu(OH)_2$ compared to calculated patterns derived from the belonging CSD entries(refcode).

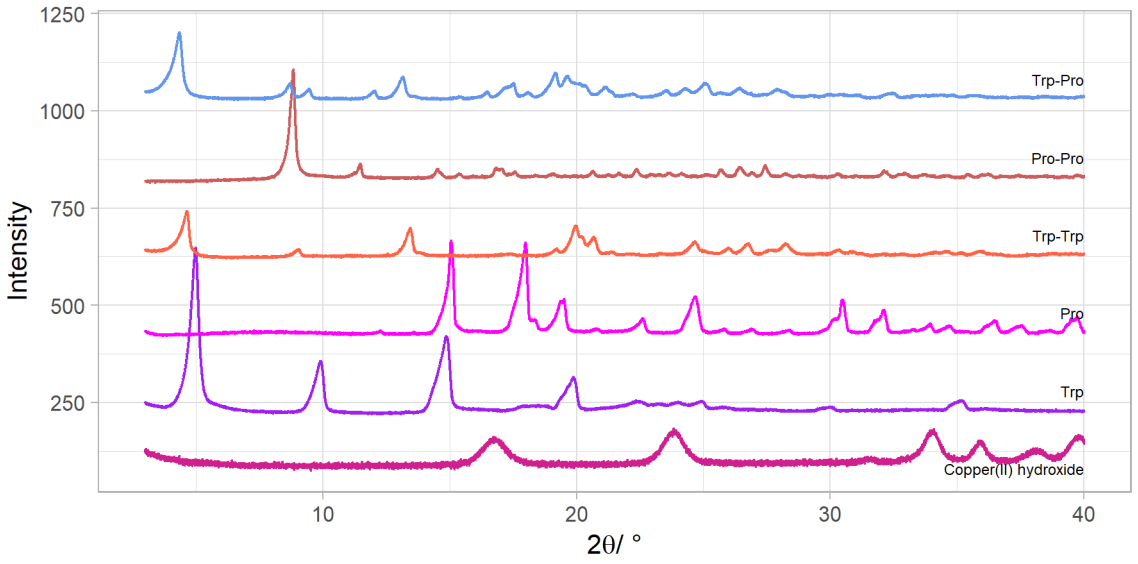

Figure S14: PXRD patterns of mechanochemically prepared samples of L-Trp and L-Pro with $Cu(OH)_2$ compared to calculated patterns derived from the belonging CSD entries(refcode).

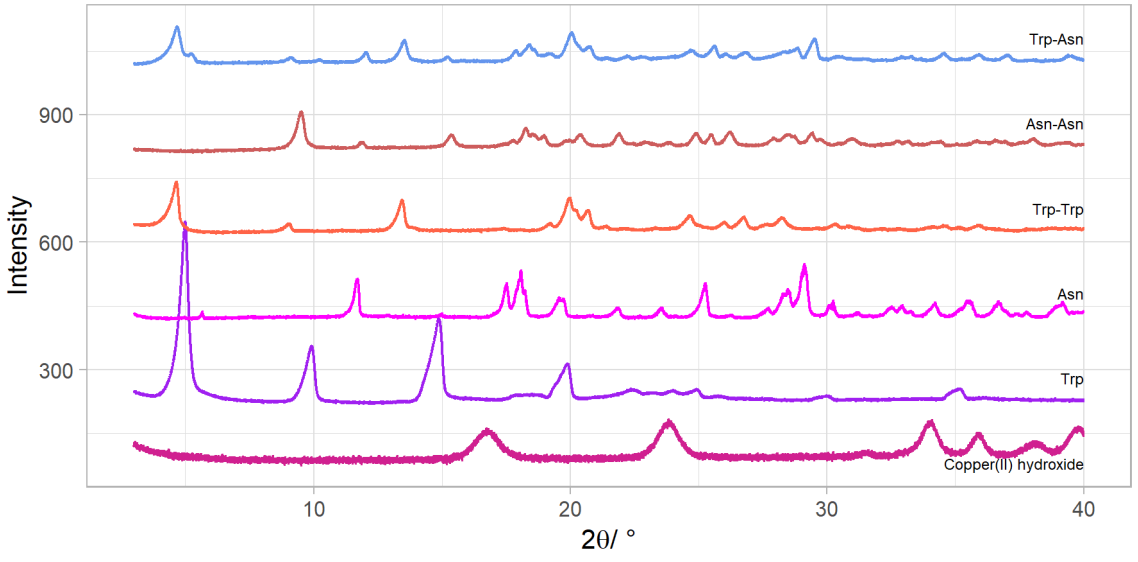

Figure S15: PXRD patterns of mechanochemically prepared samples of L-Trp and L-Asn with $Cu(OH)_2$ compared to calculated patterns derived from the belonging CSD entries(refcode).

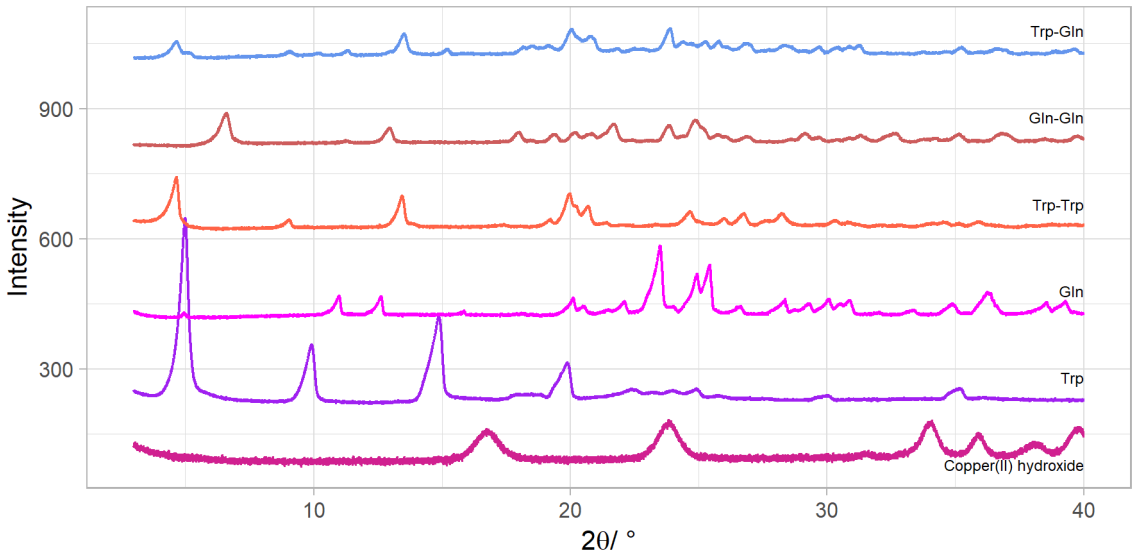

Figure S16: PXRD patterns of mechanochemically prepared samples of L-Trp and L-Gln with $Cu(OH)_2$ compared to calculated patterns derived from the belonging CSD entries(refcode).

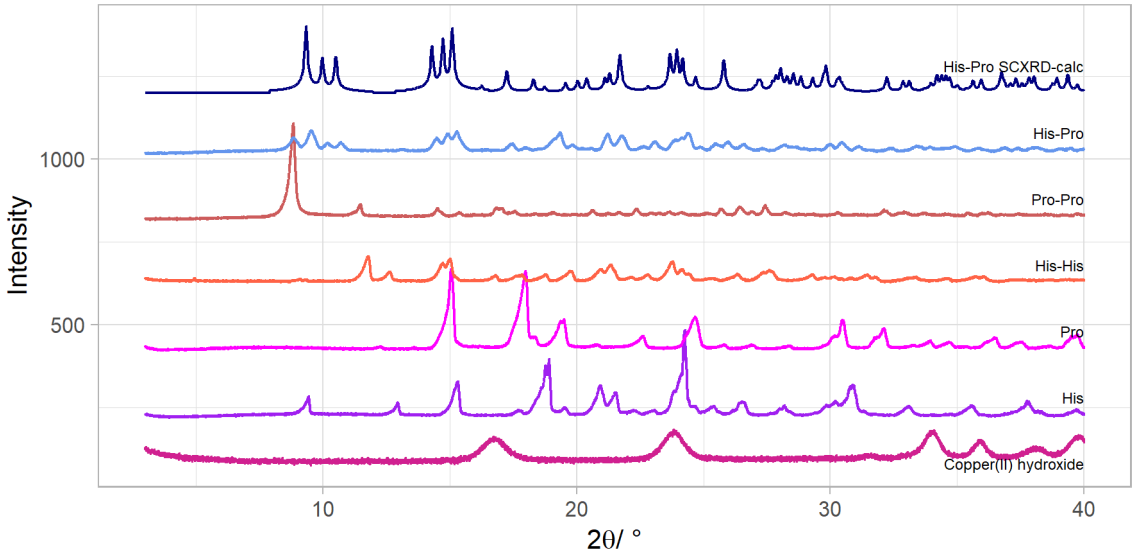

Figure S17: PXRD patterns of mechanochemically prepared samples of L-His and L-Pro with $Cu(OH)_2$ compared to calculated patterns derived from the belonging CSD entries(refcode).

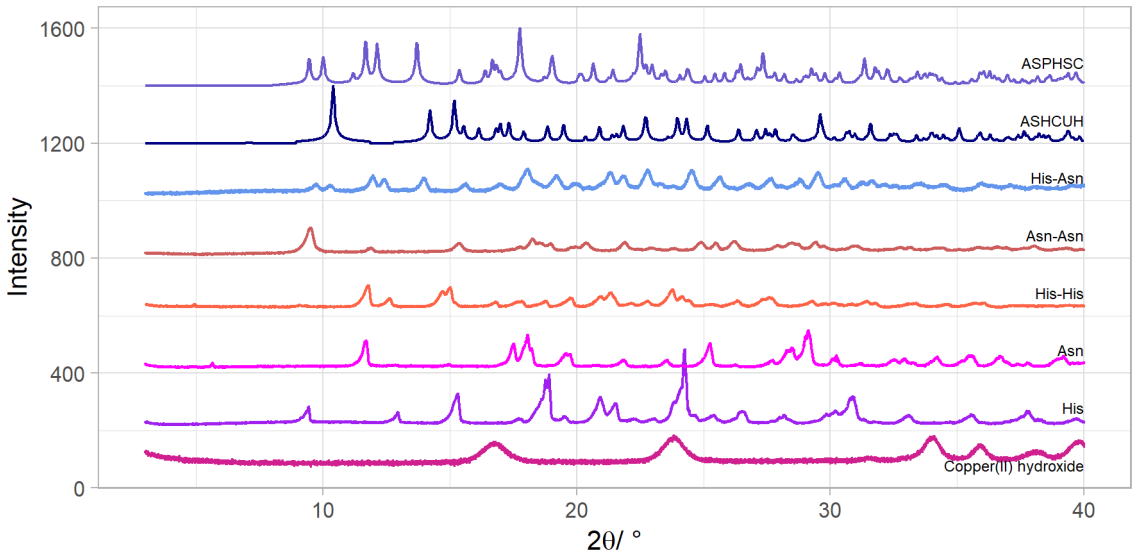

Figure S18: PXRD patterns of mechanochemically prepared samples of L-His and L-Asn with $Cu(OH)_2$ compared to calculated patterns derived from the belonging CSD entries(refcode).

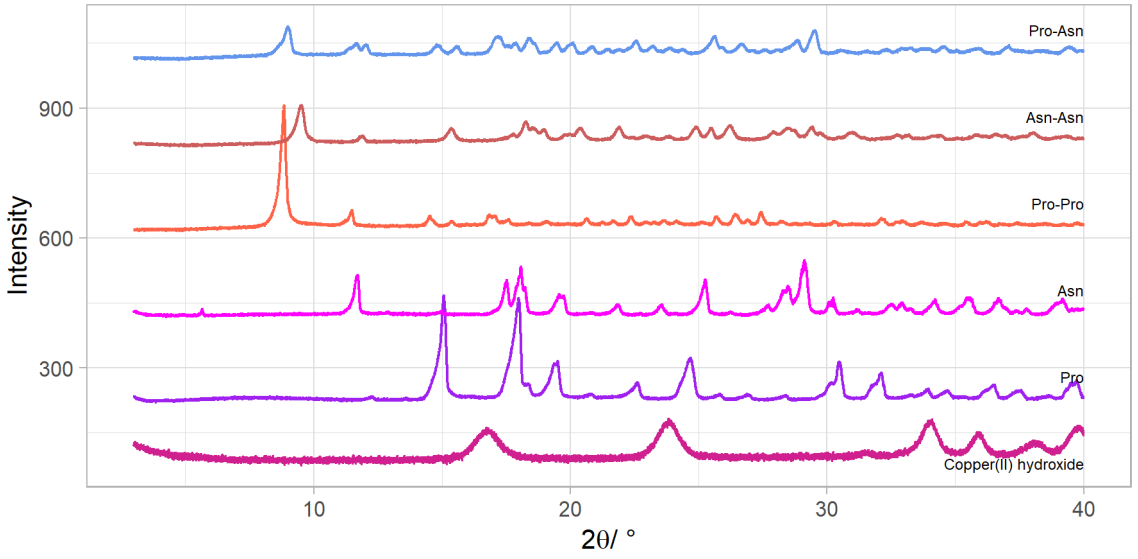

Figure S19: PXRD patterns of mechanochemically prepared samples of L-Pro and L-Asn with $Cu(OH)_2$ compared to calculated patterns derived from the belonging CSD entries(refcode).

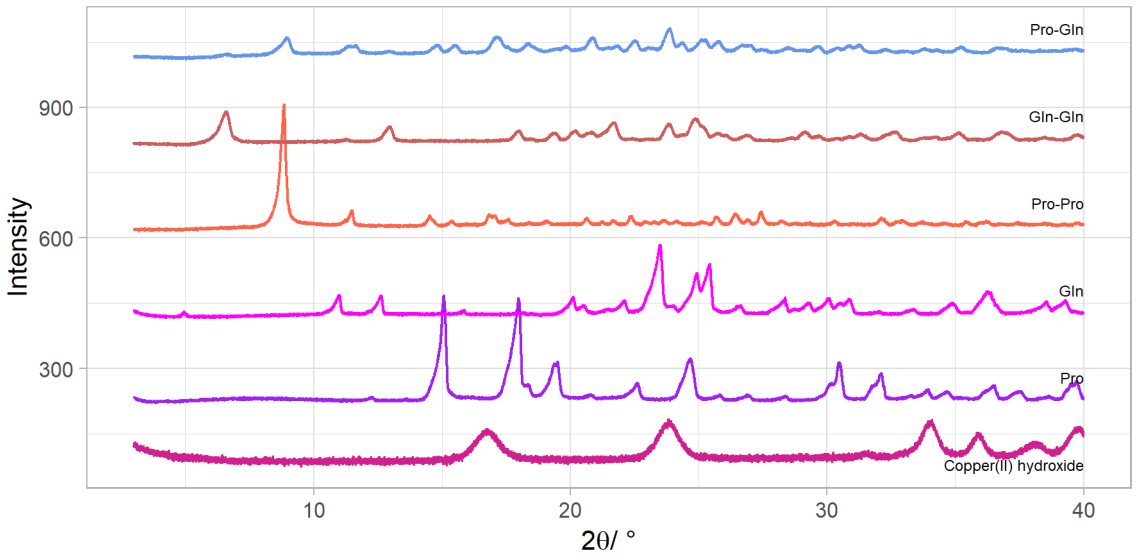

Figure S20: PXRD patterns of mechanochemically prepared samples of L-Pro and L-Gln with $Cu(OH)_2$ compared to calculated patterns derived from the belonging CSD entries(refcode).

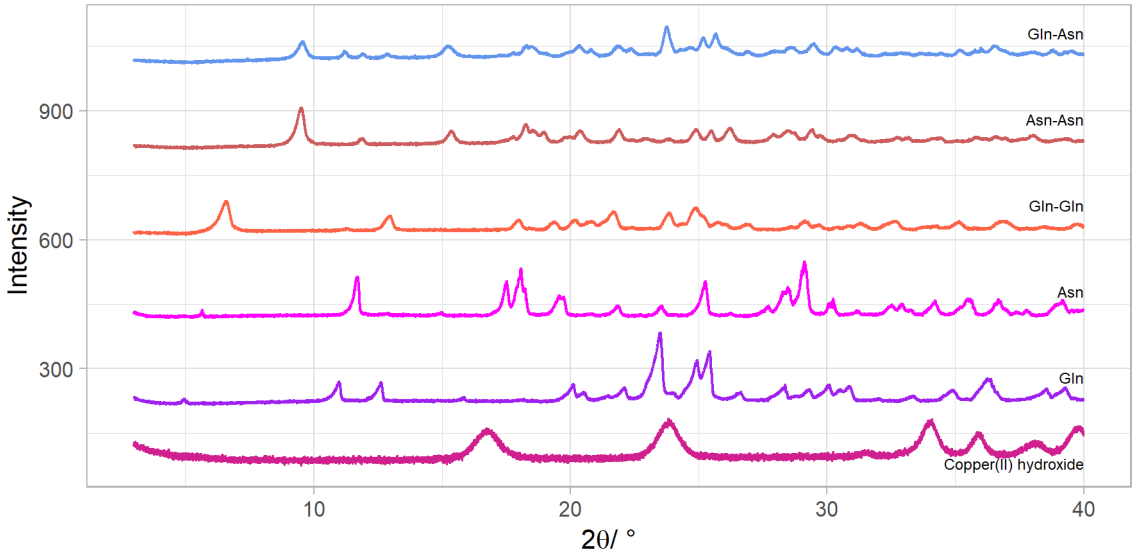

Figure S21: PXRD patterns of mechanochemically prepared samples of L-Asn and L-Gln with $Cu(OH)_2$ compared to calculated patterns derived from the belonging CSD entries(refcode).

4 References

References

(1) A. N. Agte and N. S. Golynko, *Trudy Leningr. Khim.-Tekh. Inst.*, 1940, **8**, 140.

(2) G. Brauer, *Handbook of Preparative Inorganic Chemistry V2*, Elsevier Science, Burlington, 1965, vol. 2.

(3) Rigaku Oxford Diffraction, *CrysAllispro Software system v. 1.171.40 53 64-bit*, Oxford, UK: Rigaku Corporation, 2019.

(4) G. M. Sheldrick, *Acta Crystallographica Section A Foundations of Crystallography*, 2007, **64**, 112–122.

(5) G. M. Sheldrick, *Acta Crystallographica Section C Structural Chemistry*, 2015, **71**, 3–8.

(6) O. V. Dolomanov, L. J. Bourhis, R. J. Gildea, J. A. K. Howard and H. Puschmann, *Journal of Applied Crystallography*, 2009, **42**, 339–341.

(7) A. L. Spek, *Acta Crystallographica Section D Biological Crystallography*, 2009, **65**, 148–155.

(8) C. F. Macrae, I. Sovago, S. J. Cottrell, P. T. A. Galek, P. McCabe, E. Pidcock, M. Platings, G. P. Shields, J. S. Stevens, M. Towler and P. A. Wood, *Journal of Applied Crystallography*, 2020, **53**, 226–235.

(9) Schrödinger, LLC, "The PyMOL Molecular Graphics System, Version 1.8", 2015.

(10) H. Wickham, *ggplot2: Elegant Graphics for Data Analysis*, Springer-Verlag New York, 2016.

(11) RStudio Team, *RStudio: Integrated Development Environment for R*, RStudio, PBC., Boston, MA, 2020.